

Measurement of the atmospheric neutrino energy spectrum with IceCube

Dmitry Chirkin* for the IceCube collaboration†

*University of Wisconsin, Madison, U.S.A.

†See the special section of these proceedings.

Abstract. The IceCube detector, as configured during its operation in 2007, consisted of 22 deployed cables, each equipped with 60 optical sensors, has been the biggest neutrino detector operating during the year 2007, superseded only by its later configurations. A high quality sample of more than 8500 atmospheric neutrinos was extracted from this single year of operation and used for the measurement of the atmospheric muon neutrino energy spectrum from 100 GeV to 500 TeV discussed here. Several statistical techniques were used in an attempt to search for deviation of the neutrino flux from that of conventional atmospheric neutrino models.

Keywords: atmospheric neutrinos, charm search, IceCube

I. INTRODUCTION

Most of the events recorded by the IceCube detector constitute the background of atmospheric muons that are produced in air showers. Once this background is removed the majority of events that remain are atmospheric neutrino events, i.e., (mostly) muons created by atmospheric neutrinos. Although much smaller, this also constitutes background for the majority of research topics in IceCube (e.g., extra-terrestrial neutrino flux searches), except one: the atmospheric neutrino study. As part of this study we verify that the atmospheric neutrinos observed by IceCube are consistent with previous measurements at lower energies, and agree with the theoretical extrapolations at higher energies. Since much uncertainty remains in the description of the higher energy atmospheric neutrinos, this study could provide interesting constraints on (not yet observed) charm contribution to the atmospheric neutrino production. Since such charm contribution may affect the flux of atmospheric neutrinos in a way similar to extra-terrestrial diffuse contributions, we attempt to look for both simultaneously in a single likelihood approach.

II. EVENT SELECTION

For this analysis the new machine learning method (*SBM*) described in [1] was employed. The quality parameters used with the event selection method of this paper include and build upon those discussed previously in [2]. Unfortunately the size limit of this proceeding precludes us from discussing all of the event selection quality parameters and techniques; instead we describe one new technique in detail below.

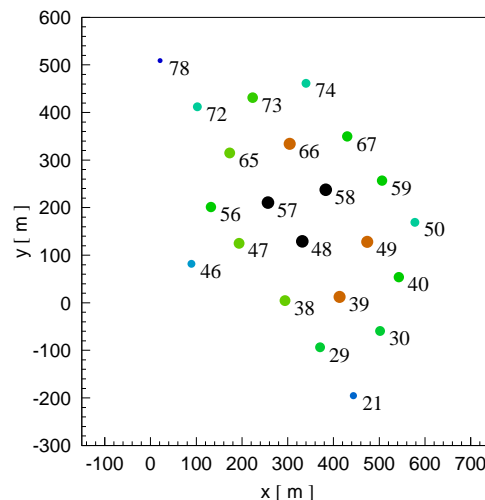


Fig. 1. View of the IceCube 22 string configuration, as used in the run of 2007. The size of the circle and color indicate the relative string weight, used to compute several quality parameters, such as the size of the veto region for contained events, or the total weight, which, much like the number of hit strings, gauges the size of an event and its importance for the analysis.

Events in IceCube are normally formed by the DAQ by combining all hits satisfying the simple majority trigger. The simple majority trigger is defined to combine all hits, which belong to one or more hit sets of at least n different-channel hits within w ns of each other. Typically $n = 8$ or more hits are required to be within $w = 5$ us of each other to satisfy this trigger.

The simple majority trigger combines hits into events only separating them in time. In IceCube a substantial fraction of events so formed turns out to consist of hits originating from two or more separate particles, or bundles of particles, typically unrelated to each other, traveling through well separated (in space) parts of the detector. In order to split up such events and to keep the rate of coincident (now in both time and space) events low, hits in the events were recombined via the use of the *topological trigger*. The definition of this trigger is very similar to that of the simple majority trigger given above: the *topological trigger* combines all *topologically connected* hits, which belong to one or more hit sets of at least n different-channel hits within w ns of each other. Two hits are called *topologically connected* if they satisfy all of the following (the numbers in *italics* show the values used in the present analysis):

- both hits originate on the detector strings

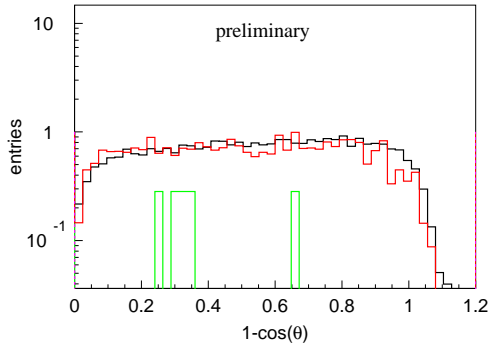


Fig. 2. Zenith angle distribution of remaining data events in 275.5 days of IceCube data (black) comparison with atmospheric neutrino prediction from simulation (red). Several double coincident air shower muon events remain at this level in simulation (shown in green). Vertically up-going tracks are at 0, horizontal tracks are at 1.

- if both hits are on the same string they should not be separated by more than 30 optical sensors
- the strings of both hits must be within 500 meters of each other
- the $\delta t - \delta r/c$ must be less than 1000 ns.

At least 4 topologically-connected hits within 4 us are required to form a topological triggered set, which is then passed through the simple majority trigger. Just like in the simple majority trigger, the hits not directly connected to each other can belong to the same event if they form topologically-connected sets satisfying the multiplicity condition with at least one and the same hit belonging to both sets.

The required distance between the strings (500 meters) was left intentionally high to allow easy scaling of the present analysis to higher-string IceCube detector configurations. Still, the rate of unrelated coincident events is much reduced via the use of the topological trigger. More importantly, the fraction of such events after the topological trigger stays at the same low level as the detector grows.

An alternative approach to recognize coincident events by reconstructing them with double-muon hypothesis was tried in a separate effort. In the present work however it is believed that the topological trigger offers several crucial advantages:

- the separation of coincident events is performed at the hit selection level
- the method is faster as it does not require complicated dual-muon fits
- not only 2 but also 3 and more coincident events can be separated
- all of these are kept for the analysis (in the alternative approach coincident events are thrown out)
- noise hits are cleaned very efficiently
- the rate of unresolved coincident events and coincident noise hits is kept at the same low level as the detector grows.

The event selection resulted in 8548 events found in 275.5 days of data of IceCube (see the 22-string config-

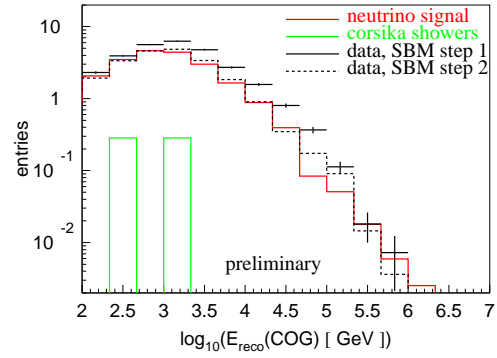


Fig. 3. Reconstructed muon energy at the closest approach point to the center-of-gravity of hits in the event. Data distribution is shown at both steps 1 and 2 of the SBM event selection method [1]. After the $\sim 90\%$ purity level is reached in simulation (step 1) it is necessary to remove more events from data that do not look like well-reconstructed muons; this is achieved by comparing data events to simulated muon neutrino events (step 2).

uration in Figure 1), or 31 events per day at $> \sim 90\%$ estimated (from simulation) purity level (contaminated by remaining atmospheric muon background). Compare this to expectation from simulation of 29.0 atmospheric neutrino events per day (Figure 2).

III. ATMOSPHERIC NEUTRINO SPECTRUM UNFOLDING

Figure 3 compares the measured muon energy distribution for conventional atmospheric neutrino simulation and data at $> \sim 90\%$ purity level. The difference between data at steps 1 and 2 of the SBM event selection is due to the presence of events that were unlike those simulated. Such events are removed at step 2 by comparing them to the events in the atmospheric neutrino simulation [1]. At this time the difference between the two data curves should be treated as a measure of (at least some of) the systematic errors introduced by our simulation.

The uncertainty in our measurement of muon energy is ~ 0.3 in $\log_{10}(E_\mu)$ in a wide energy range (from 1 TeV to 100 PeV). A larger smearing, estimated from neutrino simulation (based on [3]), is introduced when matching the muon energy at the location of the detector to the parent neutrino energy.

We tried a variety of unfolding techniques to obtain the distribution of the parent muon neutrinos, including the SVD [4] with regularization term that was the second derivative of the unfolded statistical weight; and iterative Bayesian unfolding [5] with a 5-point spline fit smoothing function (with and without the smearing kernel smoothing). Since we are looking for deviations of the energy spectrum from the power law, the SVD with regularization term that is the second derivative of the $\log(\text{flux})$ was selected as our method of choice. Additionally, we chose to include the statistical uncertainties of the unfolding matrix according to [6] (using the equivalent number of events concept as in [7]). The chosen method yielded the most consistent description of spectrum deviations that were studied;

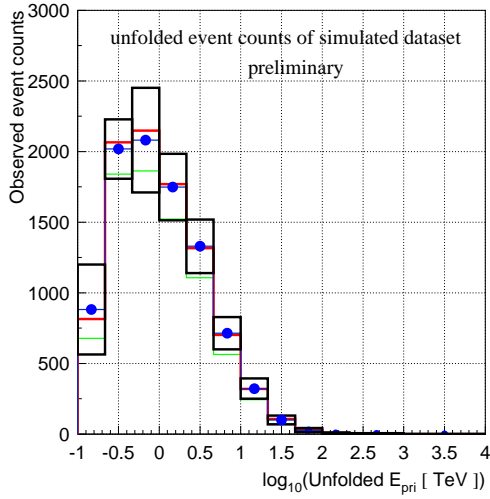


Fig. 4. Unfolded distribution of muon neutrino energies: the original distribution modeled according to [11] (red), median and 90% band of the unfolded result of 10000 simulated sets, drawn from the same simulation (blue dots/lines and black boxes, respectively). A small bias introduced by the regularization term shows up as a slight mismatch between the original and unfolded median bin values. Also shown is the distribution modeled according to [3] (green).

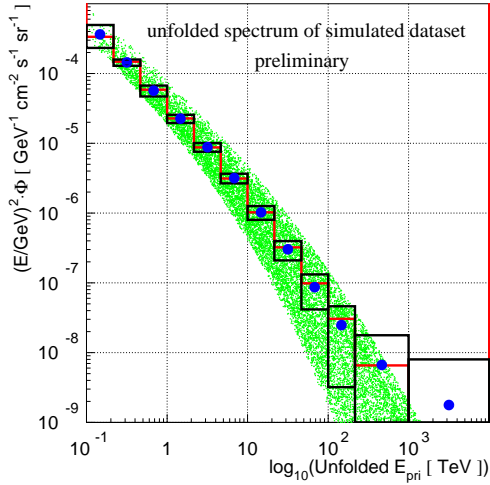


Fig. 5. Unfolded muon neutrino spectrum, averaged over zenith angle, same color designations as in Figure 4. The green points of [3] form a band as they are shown un-averaged, for each zenith angle separately.

also errors estimated from half-width of the likelihood function were reasonable when compared to the spread of unfolded results in a large pool of simulated data sets (see Figures 4 and 5).

It is possible to study the effect of small charm and E^{-2} isotropic diffuse contributions (as the two commonly studied deviations from the conventional neutrino flux models). Injecting known amounts of such contributions into the simulated event sets one computes the 90% confidence belt as in [8], [9], [10] (shown in Figure 6 for statistical weight of events in one of the bins of the unfolded distribution). The following table summarizes the average upper limits for diffuse and RQPM (optimistic) charm models (using conventional neutrino flux description as in [11]):

flux	bin 8	bin 9	bin 10	bin 11
energies, TeV	46.4–	100–	215–	1–10 PeV
E^{-2} , 10^{-8} .	5.48	3.00	3.00	4.06
RQPM (opt)	0.74	0.90	1.34	2.44

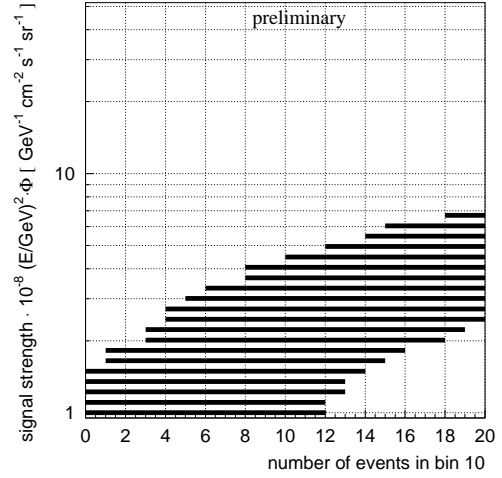


Fig. 6. 90% confidence belt for E^{-2} isotropic diffuse flux contribution, calculated with 10000 independent simulated sets for bin 10 (neutrino energies 215 TeV-1 PeV)

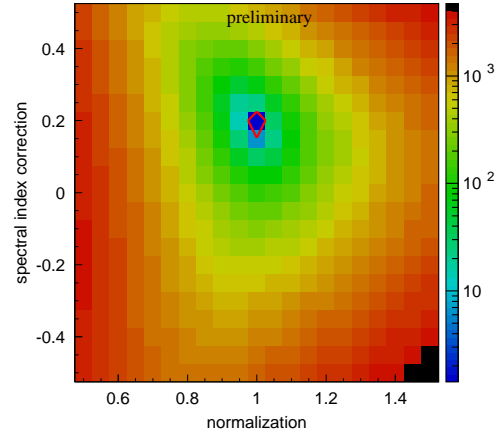


Fig. 7. Likelihood model testing profile for a simulated spectrum with spectral index deviation of +0.2 with respect to the reference model. The 90% confidence belt (shown as red contour) is very narrow and widens when systematical errors are taken into account.

IV. LIKELIHOOD MODEL TESTING

The likelihood model testing approach is well-suited to testing the data for specific deviations from the conventional flux model. This approach is based on the likelihood ordering principle of [8] and is easy employ when several deviations are tested for simultaneously [12]. This has recently been used in the analysis of the AMANDA data [13] and is also used in a similar study presented in [14].

As an example, Figure 7 demonstrates the ability to measure the deviation of the conventional flux in overall normalization and spectral index (with 8548 neutrino events in the absence of systematical errors). Figure 8 demonstrates the ability to discern simultaneous charm and diffuse E^{-2} contributions (assuming that the precise

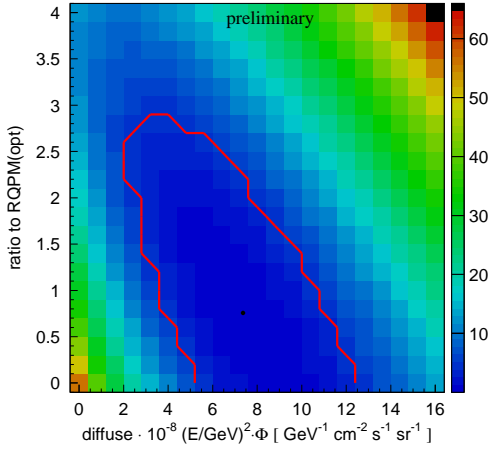


Fig. 8. A 90% confidence belt for a simulated mixed contribution of $2 \cdot \text{RQPM (opt)}$ charm expectation $+6 \cdot 10^{-8} E^{-2}$ isotropic (diffuse) component. This profile includes systematic errors on overall normalization and spectral index of the conventional neutrino flux (allowing them to vary freely).

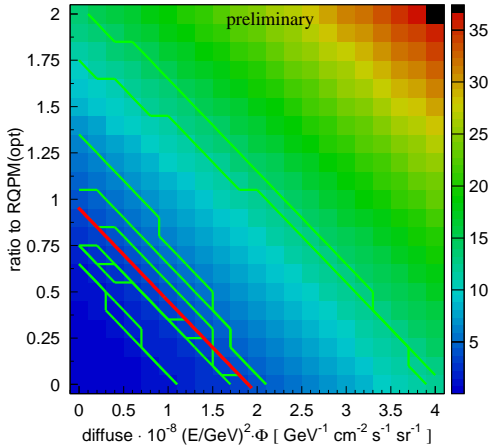


Fig. 9. 90% confidence level upper limit contours shown (in green) for 11 independent simulated data sets (drawn from the same conventional flux parent simulation according to [11]), the “median” upper limit shown in red.

normalization and spectral index of the conventional flux are also unknown). We estimate the median upper limits set by this method on both charm and diffuse E^{-2} components in Figure 9. We used the χ^2 with 2 degrees of freedom approximation to construct the confidence belts; the true 90% levels are even tighter than this (by factor $\sim 1.3 - 1.6$) due to high similarity of effects of both components on the eventual event distribution.

V. MODEL REJECTION FACTOR

This is a method that optimizes the placement of a cut on the energy observable to maximize sensitivity to an interesting flux contribution, discussed in [15]. The model rejection factor (ratio of $\overline{\mu}_{90}$ to number of expected signal events for a given flux) computed from curves shown in Figure 10 achieves its optimal value with a cut of 224 TeV on the reconstructed muon energy. The corresponding best average upper limit (sensitivity, not including systematics) of $2.14 \cdot 10^{-8}$ is achieved.

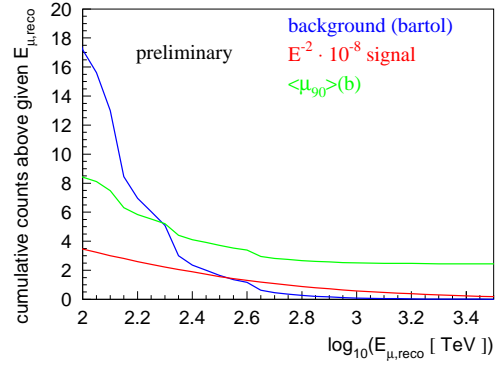


Fig. 10. Cumulative number of E^{-2} diffuse signal events shown in red, number of atmospheric neutrino events shown in blue, the corresponding average upper limit $\overline{\mu}_{90}$ is shown in green.

VI. CONCLUSIONS

We present a selection of 8548 muon neutrino events (with $\sim < 10\%$ estimated contamination from the misreconstructed air shower muon events) in 275.5 days of IceCube-22 data. An unfolding technique is selected and used to compute the average upper limit on diffuse and charm contributions. We found that the likelihood model testing and the model rejection factor methods both achieve (not surprisingly) somewhat better sensitivities.

Since the study of systematic errors is (at the time of writing of this report) not yet completed, the average upper limits presented here do not contain systematic error effects, and the actual upper limits (or the unfolded spectrum) computed from the data are not yet shown.

REFERENCES

- [1] D. Chirkin, et al., *A new method for identifying neutrino events in IceCube data*, These proceedings
- [2] D. Chirkin, et al., *Effect of the improved data acquisition system of IceCube on its neutrino-detection capabilities*, 30th ICRC, Merida, Mexico (arXiv:0711.0353)
- [3] M. Honda, et al., *Physical Review D*, V70, 043008 (2004)
- [4] V. Blobel, *An unfolding method for high energy physics experiments*, Advanced statistical techniques in particle physics conference, Durham, 2002
- [5] G.D'Agostini, *A multidimensional unfolding method based on Bayes' theorem*, DESY 94-099 (1994)
- [6] R. Barlow and Ch. Beeston, *Fitting using finite Monte Carlo samples*, Computer Physics Communications 77 (1993) 219
- [7] G. Zech, *Comparing statistical data to Monte Carlo simulation parameter fitting and unfolding*, DESY 95-113 (1995)
- [8] G. Feldman and R. Cousins, *Physical Review D*, V57, 3873 (1998)
- [9] K. Münich, J. Lünemann *Measurement of the atmospheric lepton energy spectra with AMANDA-II*, 30th ICRC, Merida, Mexico (arXiv:0711.0353)
- [10] S. Gozzini, *Search for Prompt Neutrinos with AMANDA-II*, Ph. D. thesis, Johannes Gutenberg Universität Mainz, 2008
- [11] G. Barr, et al., *Physical Review D*, V70, 023006 (2004)
- [12] G. Hill, et al., *Likelihood deconvolution of diffuse prompt and extra-terrestrial neutrino fluxes in the AMANDA-II detector*, 30th ICRC, Merida, Mexico (arXiv:0711.0353)
- [13] R. Abbasi et al. (IceCube collaboration), *Determination of the Atmospheric Neutrino Flux and Searches for New Physics with AMANDA-II*, Accepted by Phys. Rev. D., 2009, (arXiv:0902.0675)
- [14] W. Huelsnitz and J. Kelley (IceCube collaboration), *Search for quantum gravity with IceCube and high energy atmospheric neutrinos*, these proceedings
- [15] G. Hill and K. Rawlins, *Astroparticle physics* 19 (2003), 393